Weber, Jan; Schulz, Jan

Working Paper

Growing differently: A structural classification for European NUTS-3 regions

Working Paper, No. 2022-01

Provided in Cooperation with:
Department of Economics, The University of Utah, Salt Lake City

Suggested Citation: Weber, Jan; Schulz, Jan (2022) : Growing differently: A structural classification for European NUTS-3 regions, Working Paper, No. 2022-01, The University of Utah, Department of Economics, Salt Lake City, UT

This Version is available at:
https://hdl.handle.net/10419/261027

DEPARTMENT OF ECONOMICS WORKING PAPER SERIES

Growing Differently: A Structural Classification for European NUTS-3 Regions

Jan Weber
Jan Schulz

Working Paper No: 2022-01

June 2022

University of Utah
Department of Economics
260 S. Central Campus Dr., GC. 4100
Tel: (801) 581-7481
Fax: (801) 585-5649
http://www.econ.utah.edu

Growing Differently: A Structural Classification for European NUTS-3 Regions*

Jan Weber† Jan Schulz‡

June 5, 2022

Abstract

We document two novel stylized facts on European integration and cohesion. First, we show that the interregional income distribution, measured as GDP per capita at the NUTS-3 level, is bimodal for all considered years. Second, we demonstrate that this mixture of two log-normal distributions provides an excellent fit for this interregional distribution in all considered years. We put forward two meso-level interpretations of these stylized facts, based on heterodox growth theory: The log-normality of the individual clusters hints at a stochastically multiplicative process, where growth is strongly path-dependent. This can be derived from maximum entropy considerations. However, the bimodality in the income distributions also implies two separate growth mechanisms. We show that the high-variance log-normal distribution governs the dynamics at both tails of the income distribution, which might be interpreted as the core and periphery and the low-variance variant the bulk of the distribution, thus interpretable as a semi-periphery.

Keywords: Inequality; Europe; Maximum Entropy; Geometric Brownian Motion; Core; Periphery; Resilience

JEL Codes: C46, D63, F15, F43, C14, C63

*The authors would like to thank Amos Golan and Lasare Samartzidis for their valuable input. This paper benefited from the feedback we received at the Conference of the Western Social Science Association 2022 in Denver. The participation of the authors was funded by the Association for Social Economics which the authors gratefully acknowledge.

†**Corresponding Author:** jan.weber@utah.edu, University of Utah, USA

‡jan.schulz@uni-bamberg.de, University of Bamberg, Germany

1 Introduction

In 1999, eleven member states of the European Union fixed their exchange rates, a first step twards the introduction of the first Euro bills in 2002 (Raymond, 1999). To implement a common monetary within a currency area, roughly uniform development of these regions is necessary for policy to be adequate for all regions. The (newer) theory of optimum currency areas pioneered by de Grauwe (2018) has emphasized the role of shock absorption capabilities that allow for homogeneous development even in the presence of asymmetric shocks. Empirical studies on regional inequality have typically focused on correlational patterns between business cycles at the country-level. By contrast, our focus is more granular and emphasizes the role of distributional regularities at the NUTS-3 level. We document that the regional income distribution (measured as GDP per capita) is bimodal in its bulk with a long upper tail. The short time-series length for which we have complete data on European regions prohibits the use of any of the standard econometric techniques to examine growth processes. Instead, we deduce a plausible data generating process from the *stationary* distribution we observe to still shed light on the time development of European regions that we cannot directly observe (Schulz and Milaković, 2021). We show that a plausible data generating process regarding this distributional pattern is stochastically multiplicative growth composed of two volatility regimes. If we consider realized volatility to be a proxy for shock absorption capabilities, this finding highlights the role of regional resilience and multiplicative path-dependent growth. We thus provide a readily usable way to measure shock absorption capabilities that are also not directly observable. In this sense, European regions appear to be far from the benchmark, and e.g., regional convergence of fiscal policies might be necessary to homogenize shock absorption capabilities across regions and facilitate cohesion. Our major contribution based on this finding is a taxonomy of regions based rigorously on first principles that does not rely on arbitrarily fixed fractions of average EU GDP, as is now used in EU cohesion policy (European Parliament and Council of the European Union, 2021).

Traditional dependency theory emphasizes the taxonomy of countries falling either in the 'core' or in the 'periphery', with the economic development in the periphery being "conditioned by the development and expansion of" the core (Dos Santos, 1970, p. 231). The main hypothesis is that this asymmetry is due to differences in the industrial composition of core and peripheral countries: While peripheral countries tend to produce primary goods like raw materials that are rather easily substitutable, the core countries produce sophisticated industrial products with much less scope for substitution. This leads to much more intense competition for peripheral than for core countries, letting the terms of trade for the periphery deteriorate. They receive less and less manufactured goods in (unequal) exchange for their primary goods (Prebisch, 1950; Singer, 1950).

We build on this classification to argue that primary goods producers face much more volatile growth paths than industrial producers since they are also much more exposed to fluctuations in world market prices. We argue further that highly developed producers with high output might also face volatile growth, since their production of, e.g., cars is based on long and diversified supply chains (Acemoglu et al., 2012; Elliott et al., 2022). Financial hubs might also face rather high volatility, since financial markets are typically much more volatile than 'real economy' markets.

However, while typical studies on core-periphery patterns typically rely on country-level data, we focus on European regions. This is an attempt to answer the "challenge of granularity" (Gräbner and Hafele, 2020, p. 7), i.e., the problem that the country level of aggregation masks important heterogeneity at the subnational level. Most prominently, as our analysis will also show, some regions in the North of Italy can plausibly be defined as part of a highly industrialized core, while the Southern 'Mezzogiorno' is not as developed and can thus more plausibly considered to be peripheral. Our results highlight that this is indeed an important oversight of country-level studies with the success of common monetary policy crucially relying also on homogeneous development *within* countries. Our rigorous taxonomy might thus aid in tailoring policies for specific regions and regional development.

Our analysis focuses on differences in the second moment of growth rate distribution by assuming equal expected growth rates. We show that this parsimonious assumption in conjunction with multiplicative growth gives rise to the observed distributional patterns. The assumption of multiplicative growth is sufficient to generate a strongly skewed distribution of GDP levels, as it features a rich-get-richer phenomenon and, thus, path-dependent growth (Gibrat, 1931; Kalecki, 1945). Random multiplicative growth also known as the *law of proportionate* effect in the literature (Gibrat, 1931) implies that the expected growth rate of a given region does not depend on its GDP, i.e., growth is scale-independent. Scale-independent growth is for example, explained by capital reallocation with capital flowing to regions with excess profit capabilities and thus equalizing rates of return and thus a reasonable starting point (Schulz and Milaković, 2021). Our explanatory attempt thus focuses not only expected growth but growth volatility. This is not to say that the traditional explanations within dependency theory focusing on first moments are necessarily false when applied to the regional level. We only argue that volatility and the ability of regional economies to absorb shocks are very fruitful and neglected dimension to explain interregional disparities.

The remainder of this paper is organized as follows: In section 2, we introduce our basic theoretical models and show how both a Geometric Brownian motion with heterogeneous volatility components and a maximum entropy program leads to a mixture of two log-normal components. In the following section 3, we describe the dataset we use to test our theoretical predictions and our estimation methods. We apply these methods in section 4 to show that we indeed find a mixture of two log-normal densities for the overall distribution of regional EU GDP per capita levels that can be used to rigorously categorize regions into a core, semi-periphery, and periphery region. We conclude and discuss the implications of our findings in the final section 5.

2 Model

2.1 Geometric Brownian Motion

The above qualitative discussions lend themselves to being formalized as growth following two distinct Geometric Brownian Motion (GBM) processes. Path-dependent growth characterized by the multiplicative dynamics, while the structural taxonomy according to core, semi-periphery, and periphery implies different volatility regimes. In particular, both core and periphery are assumed to follow growth processes with relatively high volatility, albeit for very different reasons: While the core counties exhibit industrial structures with a focus on finance, natural resources, and the automotive sector, the reliance of peripheral counties on raw materials and thus world prices make those growth processes more volatile.

We formalize this argument by postulating that core and peripheral countries i follow a GBM process H with high volatility. In contrast, semi-peripheral counties j follow a GBM process L with low volatility. Assuming equal drift terms μ for simplicity, this implies these two differential equations:

$$dY_i^H(t) = \mu Y_i^H(t) + \sigma^H dW_t \tag{1}$$

and

$$dY_j^L(t) = \mu Y_j^L(t) + \sigma^L dW_t, \tag{2}$$

with $t \geq 0$, W as Wiener increments and $\sigma^H > \sigma^L$

$$. \tag{3}$$

Since the stationary distribution of any Y for any initial value $Y(0)$ with t sufficiently large converges to a log-normal distribution (Gibrat, 1931; Kalecki, 1945), we expect that the resulting distribution of our economy characterized by $N^H \in \mathbb{N}$ counties of type H and $N^L \in \mathbb{N}$ counties of type L will follow a mixture of two log-normals. The higher volatility in

the growth of type H counties by $\sigma^H > \sigma^L$ will eventually manifest as counties being pushed towards the upper and lower tails of the overall distribution of Y, with the low volatility counties populating the remaining segment between these two tails. This is what we indeed observe simulating a discretized version of (1) and (3) with $N^H = N^L = 500$, initial value equal for all i and j as $Y(0) = 1$, $\mu = 0.01$, $\sigma^H = 0.3$ and $\sigma^L = 0.05$ after $1,000$ time steps.

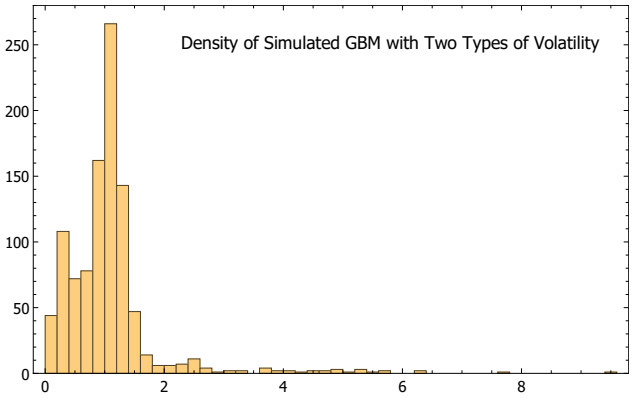

(a)

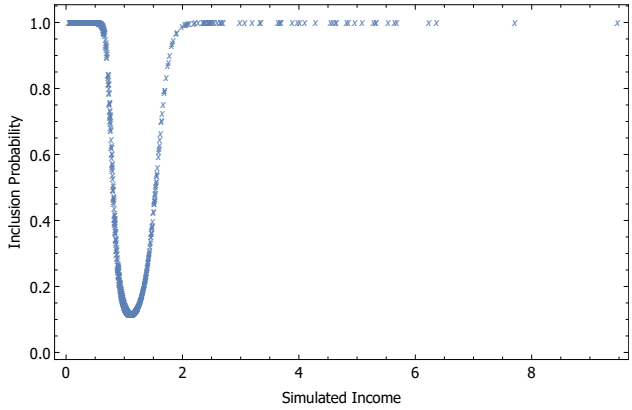

(b)

Figure 1: The density of simulated GBM with two volatility types (left panel) and the inclusion probability in the estimated log-normal component with high variance.

2.2 Maximum Entropy

The Maximum Entropy approach, introduced by Jaynes (2019) and based on Shannon (1948), differs from the traditional methods in economics. Any researcher who wants to derive a distributional form for a variable must explicitly state all underlying assumptions contribut-

ing to the model. This transparency is not only necessary for the approach itself; it is also honest towards the research community as it discloses all theories and contributes to full transparency. Only explicitly stated assumption find their way into the final functional form as Maximum Entropy leads to the least-informed possible distribution.

Based on a first visual inspection of the data, the bimodality of the GDPpc distribution is striking. Therefore, we consider a two-component mixture distribution to adequately capture the underlying data generating process. The Gaussian distribution of the logarithmic GDPpc appears to be particularly plausible as it comes from two important properties of the area under observation. First, we rule out that GDPpc in itself is the result of additive growth: Income levels are not reassigned for every period but rather depend on the level in previous periods, indicating the relevance of capabilities that are already in place. Second, as long as this *multiplicative* growth process has a finite variance in growth rates without any further constraints (Thurner et al., 2018), we will observe a log-normal distribution. Even when growth rates are mesokurtic, the resulting stationary distribution features a fat tail.

As Shannon's entropy is defined by

$$H(x) = -\int_{-\infty}^{\infty} p(x) \times \log p(x) dx, \tag{4}$$

and the probability density $p(x)$ has to integrate to unity, the Maximum Entropy problem is well defined and can be solved by applying a Lagrangian.

$$\mathcal{L}\left(p(x), \lambda_i\right) = -\int_{-\infty}^{\infty} p(x) \times \log p(x) dx - \lambda_1 \left(\int_{-\infty}^{\infty} p(x) dx - 1\right) \tag{5}$$

$$- \lambda_2 \left(\int_{-\infty}^{\infty} p(x) \log x dx - \mu\right) - \lambda_3 \left(\int_{-\infty}^{\infty} p(x) \left(\log x - \mu\right)^2 dx - \sigma^2\right) \tag{6}$$

$$= H\left(p^{\star}\left(x\right)\right) \tag{7}$$

Apart from the normalization constraint for all probability density corresponding to λ_1, the

two constraints with Lagrange multipliers λ_2 and λ_3 relate to the logarithm of the random variable x or GDPpc in question and thus to the relevant growth rates. The two constraints with multipliers λ_2 and λ_3 can thus be interpreted as defining a common expected rate of growth (constraint no. 2) and the growth rate distribution having fixed finite variance (constraint no. 3). We show in Appendix A that this optimization problem is solved by the probability density function $p(x)$ of a log-normal distribution. Here we also show that the standard deviation of growth rates expressed in constraint no. 3 relates directly to the standard deviation of the emerging log-normal distribution, much like for the GBM specification. The mixture of two log-normal densities thus also emerges for the maximum entropy programme, whenever we suppose differently volatile stochastically multiplicative growth processes.

If we were to change the constraints for the maximum entropy program, we derive a different distributional form (Golan, 2017). Assuming that the data has a well-defined finite mean and variance would, for example, lead to a Gaussian normal distribution. If we remove the assumption of a well-defined variance to allow for a large variation in the data and require the data to be positive, we would derive the exponential distribution. Since all of the here presented options are plausible, we test all six combinatorial possibilities to fit the data.

As the Principle of Maximum Entropy is not just compatible but rather an overarching framework for Bayesian analysis, we estimate the models using Bayesian methods (Giffin and Caticha, 2007). We provide the 95% credibility interval for all estimations if not stated differently.

Applying the maximum entropy approach to empirical data, the outcome of political decisions and evolutionary trends provides a researcher with a broader range of analytical tools than a frequentist or Bayesian analysis could do. As the observed (and estimated) distribution is the one maximizing entropy, we know that our model is complete and does not lack essential features. A supra-national entity that would (or at least attempt to) redistribute all income equally over all people would counteract the systemic development and

lead to a different distributional form, but not change the fundamental dynamics themselves. This has far-reaching consequences for any political discussion and analysis as resources must be invested to overcome the current state and development if desired (Abel, 2014).

We classify constraints as systemic but policy measures as changes within the system. The constraints of a system are general and define the environment in which political decisons can be made. An analogy for this would be a car racetrack: The conditions of the system define the track, guardrails limit the possibilities of what is possible for the cars. Regulations, however, define the rules of the race as they set speed limits and define unsportsmanlike behavior. How the cars and driver behavior on the racetrack therefore depends on the systemic conditions and in-system regulations. Similar reasoning can be applied to our understanding of the EU regional system: Regions develop according to fundamental constraints that we interpret as reflecting different industrial compositions, leading to differences in realized volatility. We consider these to be systemic. Policy can directly intervene by redistributive measures but will have to do so in every period, since the fundamental constraints will lead the system to the same stationary distribution we observe. Only industrial policy that focuses directly on industrial composition and specialization patterns has the potential to change these fundamental constraints, making constant redistribution perhaps less necessary. We will return to this aspect in Section 5.

3 Data and Method

The European Union provides exhaustive data for the socio-economic environment in its member states and regions. This data is available at different levels of granularity to allow for an improved and coherent insight across all members, candidates, and countries that are part of the European Free Trade Agreement (EFTA). Those NUTS[1] levels define the level of disaggregation. While NUTS 1 includes the whole country for smaller countries, larger countries are separated into several NUTS-1 regions. France, for example, reports for 14

[1]Nomenclature des unités territoriales statistiques

regions and oversea departments, Germany for its 16 states. NUTS-2 is the next smaller administrative level, and NUTS-3 is the smallest non-local administrative unit. For most countries, data available on NUTS 3 level represents county-level data.

In our analysis, we rely on the Gross Domestic Product data at market prices per capita (GDPpc) on a NUTS-3 level. The data has been downloaded from the official Eurostat homepage and is labeled with the data-code *nama_10r_3gdp*. For consistent estimates, we concentrate on a coherent period of time for which data coverage does not change. As for nearly all departments in France data for 2014 and before is not available, and data for 2019 and later has in general not been released, our analysis concentrates on the years 2014-2018. Those years also represent a relatively quiet period of macroeconomic shocks on the European continent, covering the time between the debt crisis and the turbulent and unprecedented times of Covid-19.

For all our estimations, we use the R-package *rstan*, provided by the Stan Development Team (2021). In a first step, we determine the most likely structural form for the distribution of GDPpc. We provide standard econometric tests and informational indicator to specify which model suits the available data best. As we can identify the bimodal empirical distribution as a two-component mixture distribution, we can assign each NUTS 3 region based on Bayes Theorem a probability to belong to one or the other component. In a third and final step, we use the characteristics of a region with respect to its volatility regime and absolute value in GDPpc to provide an indicator for the different clusters of core, semi-periphery, and periphery. To our knowledge, such a county-level indicator based on empirical data has not been presented in the literature yet.

4 Results

4.1 One Mixture

As previously mentioned, we estimate a two-component mixture distribution based on the visually observed bimodality. We test the assumptions of two log-normal, two normal, two exponential, and the mixture of two different distributions against the empirical data. Overall, this gives us six possible theoretical distributions as the testing procedure remains agnostic about the order in which those distributions may appear.

It is not our goal to verify a predetermined assumption about the nature of the data but rather derive the most likely solution. Table 1 presents our effort to test all six possible distributions against the empirical data. We concentrate on the most common tests in the statistical literature, the Kullback-Leibler divergence (KLD), Kologoroff-Smirnov (KS), Anderson-Darling (AD), Cramér-von Mises (CvM), as well as AIC and BIC to account for the different amount of parameters in the models.

For nearly all years and tests, the two log-normal mixture model (LN/LN) provides the most accurate description for the underlying data. The fit of the LN/LN remains statistically significant for all years and tests at the 1 percent significance level (see Table 2). This significance level is also achieved for the two cases where the AD test prefers the mixture of two Gaussian distributions above the LN/LN model.

	KLD	KS	AD	CvM	AIC	BIC
2015	LN/LN	LN/LN	LN/LN	LN/LN	LN/LN	LN/LN
2016	LN/LN	LN/LN	N/N	LN/LN	LN/LN	LN/LN
2017	LN/LN	LN/LN	LN/LN	LN/LN	LN/LN	LN/LN
2018	LN/LN	LN/LN	N/N	LN/LN	LN/LN	LN/LN

Table 1: In 22 out of 24 cases, the mixture of two log-normal distributions provides the best fit to the empirical data.

Estimating the parameter for all four years shows minor fluctuations of the distributional form throughout the years. Especially the mixing parameter θ remains roughly constant,

indicating that no significant disturbances to the structure of the economic environment occurred. Analyzing a longer time period might be beneficial to address structural developments that are beyond this paper's scope. Figure 2 illustrates the different location of the two components and the previously introduced stylized fact of two different variances, significantly higher for the first component. This testifies to the robustness of our argument that also implies stable economic conditions based on volatility.

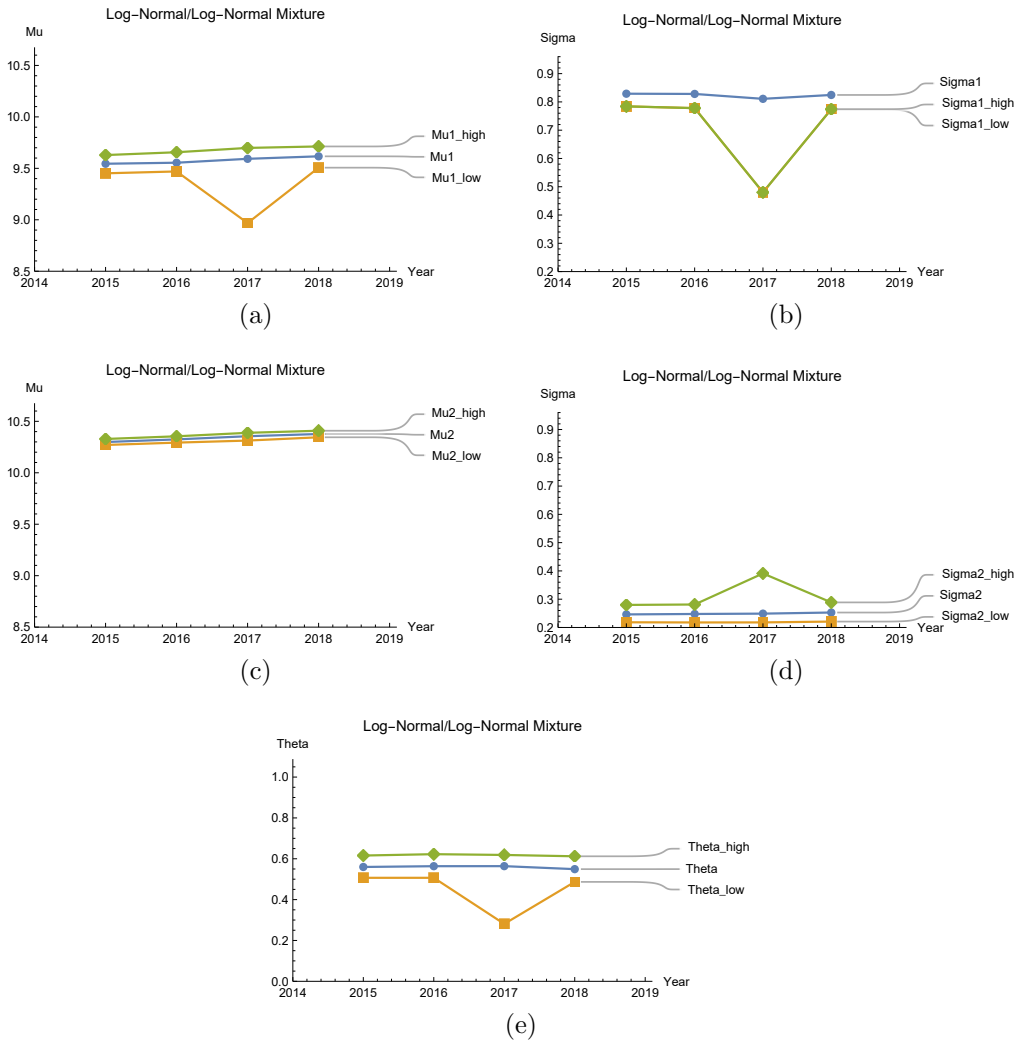

Figure 2: The parameter over time for the first LN component (top), the second LN component (middle), and mixing parameter (bottom). We also provide the 95% credibility interval to outline the stability and significant differences between the two components.

Besides providing statistical evidence, we want to highlight the accuracy of the LN/LN

	KS		AD		CvM	
2015	0.342232	(***)	0.467545	(***)	0.59341	(***)
2016	0.437714	(***)	0.465474	(***)	0.597986	(***)
2017	0.379998	(***)	0.339621	(***)	0.43011	(***)
2018	0.499479	(***)	0.437892	(***)	0.63037	(***)

Table 2: For none of the years and selected tests, the mixture of two log-normal distributions can not be rejected at a 1 percent significance level.

model compared to the empirical data in Figure 3. The theoretical fit of the LN/LN model is striking, showing that our model indeed seems to capture the empirical data-generating process well.

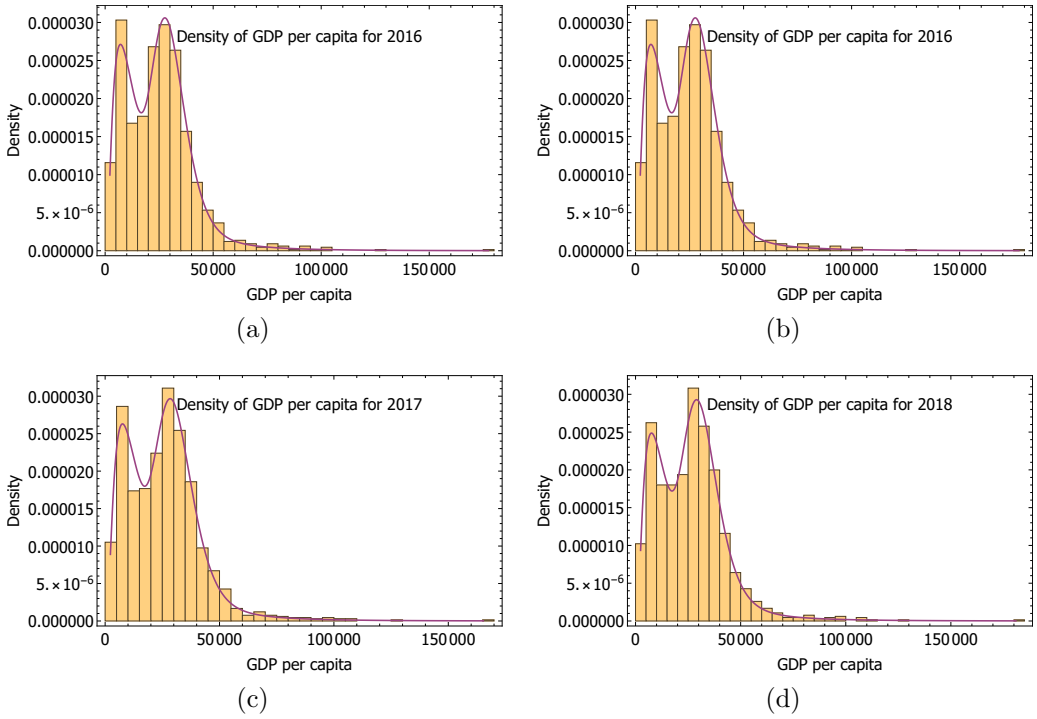

Figure 3: The densities of GDPpc for all regions with fit for log-normal-log-normal mixture (2015 – 2018).

4.2 Two Regimes of Volatility

Since we observe a two-component mixture for one dataset, assigning each observation a probability to be part of one of those two distributions is possible. As we know that a

specific region is part of the dataset, we also know that the probability that region A is in distribution LN1 is the counterprobability that the region is in distribution LN2. This allows us to assign each region to a probability regime based on the likelihood that the specific region belongs to the underlying distribution. In a final step, we assign an observation to the distribution to which it more likely belongs, implying a cut-off probability of 0.5.

Inspired by the work of Scharfenaker and Semieniuk (2015), we apply Bayes' theorem to determine to which component of the mixture distribution (LN1 or LN2) each observation c belongs:

$$p(LN1|c) = \frac{p(c, LN1)}{p(c)} \tag{8}$$

$$= \frac{p(LN1)p(c|LN1)}{p(LN1)p(c|LN1) + p(LN2)p(c|LN2)} \tag{9}$$

$$= \frac{\phi_1 LN(c|\mu_1, \sigma_1)}{\phi_1 LN(c|\mu_1, \sigma_1) + \phi_2 LN(c|\mu_2, \sigma_2)} \tag{10}$$

As we estimated the parameter of the mixture distribution, it is straightforward to plug in the estimated values and determine the probability for each observation belonging to LN1 and LN2 vice versa. What we observe for all years is a U-shaped relation between the GDPpc and probability belonging to LN1. Figure 4 illustrates how regions with a high or low GDPpc belong to LN1, while regions with a medium-range GDPpc belong to LN2.

As shown in Section 2.1, this indicates that two regimes of volatility must classify the NUTS 3 regions in Europe. A high volatility cluster consisting of low and high GDPpc, separated by a low volatility cluster covering the middle GDPpc regions.

4.3 Three Clusters of Inequality

In a final step, we consider the two regimes of volatility and the absolute value of GDPpc for the NUTS 3 regions in Europe to determine a data-driven indicator for a small-level separation into core, semi-periphery, and periphery. As we have separated all regions into two

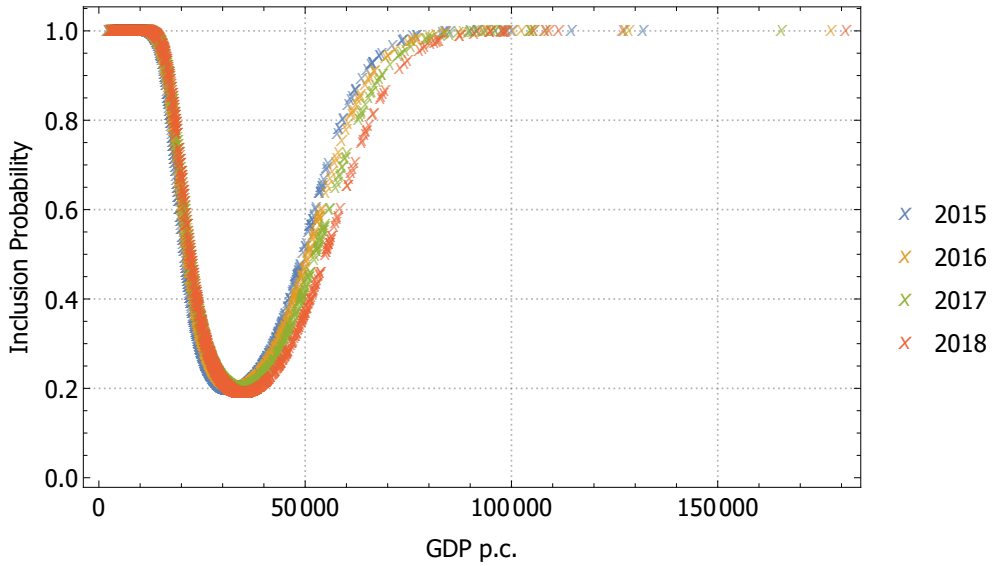

(a)

Figure 4: Probability of each region to be part of LN1, depending on income. For all four years, we see a clear U-shaped behavior.

regimes of volatility in the previous step, we use of the fact that high and low GDPpc regions are in the same component of the mixture model. We, therefore, classify high volatility/high GDPpc regions as the core, low volatility regions independent of their GDPpc as semi-periphery, and high volatility/low GDPpc regions as periphery. We, therefore, use the ends of the U-shaped graph to indicate periphery and core, which are, in line with the literature (Zhao, 2021), separated by the semi-periphery in the lower U-shape of the graph.

This allows us to present a data-driven overview of the regional European economic structure. For an optimal visual representation, Figure 5 is color-coded, representing the different structural components[2].

Regions that are classified as the core come with considerably more petite surprise. Their high degree of integration into the world economy through their leading economies like finance, automotive sector, or oil, a high GDPpc comes to the cost of high volatility. Examples here are Luxembourg, Wolfsburg, Munich, and Milano. The industrial compositions of these regions are perhaps equally outward-looking than the peripheral ones and dependent on

[2]We would like to thank Milos Popovic for providing the code for this and many more maps on his homepage: https://milospopovic.net/

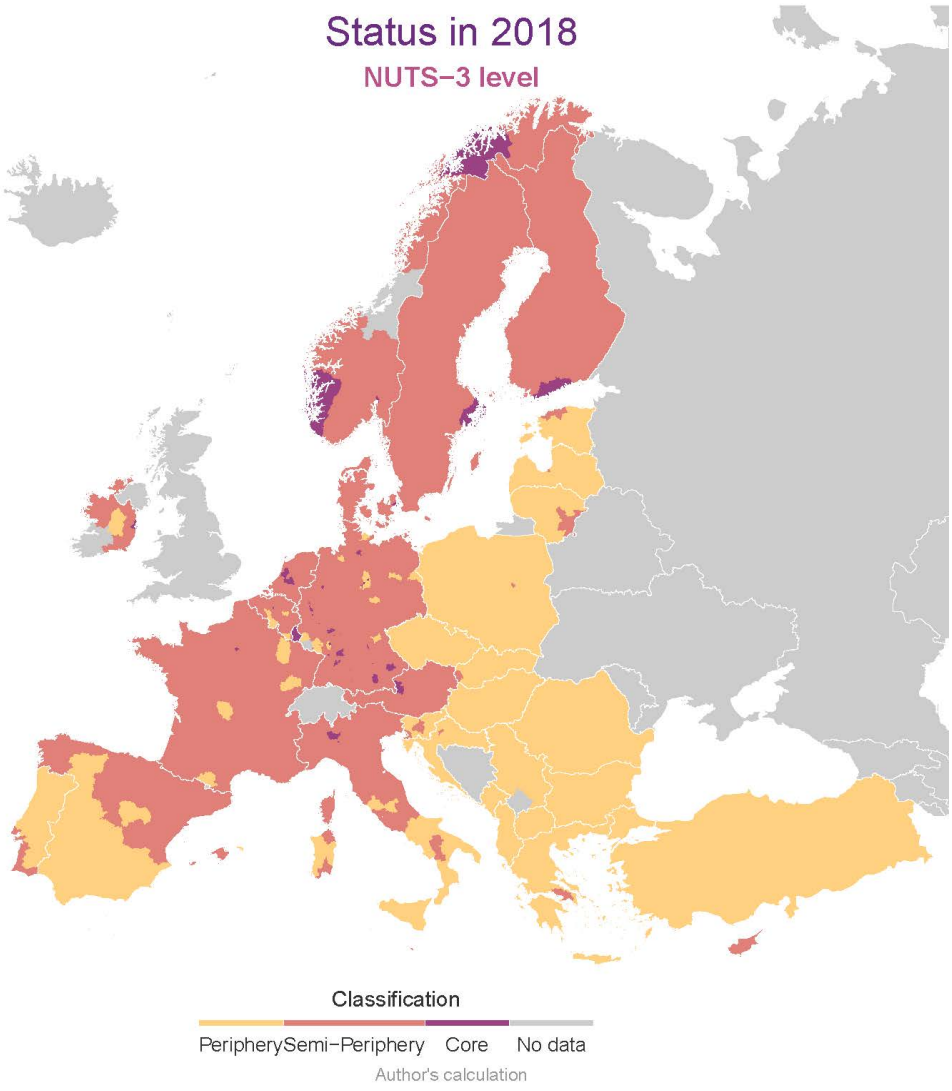

(a)

Figure 5: Visualization of the regions under consideration and their classification into core, semi-periphery, or periphery for the year 2018. The maps for all other years under consideration are presented in Appendix B, as low variation over time can be observed.

international commodity and capital markets. However, these regions appear to be net beneficiaries from the relatively high induced volatility. Particularly those regions specializing in financial products should experience volatile growth paths since volatility in financial markets is typically one order of magnitude higher than in commodity or service markets

(Mundt et al., 2014). The semi-periphery, however, is composed of regions in central Europe that are known for their high economic performance but not necessarily for specialization into a specific product. A larger variety of industries in those regions might balance external shocks from the world market in individual industries. It is also possible that these regions do not feel the same exposure to world market shocks to the core industries, as their involvement in those industries is secondary by purely supplying input factors. Finally, the peripheral countries will tend to produce primary products and are thus much less able to absorb external shocks. This is because substitutability of primary goods is generally high, leaving producers of these goods with a relatively low market power and thus very exposed to price developments on the world market (Prebisch, 1950; Singer, 1950).

5 Discussion and Political Implications

The short period of observation does not allow for an in-depth evaluation of the efforts by the European Union to create parity in living standards. It does, however, allow for warnings towards any such policies. It is crucial to take the different characteristics in Europe into account and how those regions are connected. Besides the GDPpc for a region, it is important to consider the volatility this region faces in its economic structure. A region in the south of Spain might be more similar to Poland rather than a region in the north of the country with respect to the structural foundation. This different capability to absorb economic shocks within a single country, but similar capability to other regions in Europe must be incorporated into any economic policy.

While much of the literature has focused on the expected rate of growth on a national level (Gräbner et al., 2020), our approach is more granular. It underlines the importance of the second moment of growth rate distributions, i.e., volatility. We show that stochastically multiplicative growth, either formalized by a Geometric Brownian Motion or by solving the corresponding maximum entropy program, can replicate the observed distributional patterns

with the minimal additional assumption that there are structural differences in volatility between regions. Our reduced-form representations are far from a full-fledged growth model; still, we argue that such a full-fledged regional growth model must be *observationally equivalent* to the stochastic representation we propose.

As previously mentioned, the applied Maximum Entropy and GBM approach rejects any potential claims that the current political framework of the EFTA ensures or even promotes a uniform standard of living across its regions. As the observed distribution is derived under the assumption of GDPpc which depends on and mesokurtic developments of income level, a redistribution effect that correlates with the GDPpc in a specific region can be ruled out. Such a redistribution would essentially amount to progressive taxation. This becomes intuitively clear when considering the implications of the Maximum Entropy approach as under the given constraints, no other emergent stationary distribution than a log-normal distribution is possible. For our postulated theoretical data-generating process, any specific realization of growth rates will eventually (asymptotically) diverge to a log-normal distribution.

This point cannot be stressed enough, as it highlights the difference between systemic and within-system changes. While constant redistribution does not address the fundamental data-generating process, it changes the outcome by active intervention. If the process of redistribution ends, the distribution of GDPpc will again be (asymptotically) log-normal. This observation lends itself directly to a taxonomy of policy measures: Any temporary redistributive scheme will not change the systemic nature of the growth process with the log-normal as an attractor and is thus fundamental unable to provide equality across regions. By contrast, policies that alter the constraints of the system, e.g. by appropriate industrial policy or an entrepeneurial state activity, can in principle generate any stationary distribution of regional income levels. Our results suggest that such changes to the system have to address the capability to absorb shocks in all NUTS 3 regions by equalizing the industrial composition and therefore the volatility regime.

Our investigation has not just provided new and additional insight into the inequality between different regions in Europe but also contributes to the problematic and often coarse-grained differentiation of regions into growth and performance-orientated regimes. Specifically, we provide a data-driven approach that classifying all regions on a NUTS 3-level in a core, semi-periphery, and periphery framework. We hope that our work will contribute to more informed discussion and policies to achieve a more uniform standard of living in Europe.

References

Abel, C. (2014). Various Properties of the Log-Normal Distribution. Technical report.

Acemoglu, D., Carvalho, V. M., Ozdaglar, A., and Tahbaz-Salehi, A. (2012). The Network Origins of Aggregate Fluctuations. *Econometrica*, 80(5):1977–2016.

de Grauwe, P. (2018). *Economics of Monetary Union*. Oxford University Press, United Kingdon.

Dos Santos, T. (1970). The Structure of Dependence. *American Economic Review*, 60(2):231–36.

Elliott, M., Golub, B., and Leduc, M. V. (2022). Supply Network Formation and Fragility. *arXiv:2001.03853 [physics]*.

European Parliament and Council of the European Union (2021). Regulation(EU) 2021/1060 of the European Parliament and of the Council.

Gibrat, R. (1931). *Les Inégalités économiques*. Recueil Sirey, Paris.

Giffin, A. and Caticha, A. (2007). Updating Probabilities with Data and Moments. *AIP Conference Proceedings*, 954:74–84.

Golan, A. (2017). *Foundations of Info-Metrics: Modeling and Inference with Imperfect Information*. Oxford University Press, New York, NY.

Gräbner, C. and Hafele, J. (2020). The emergence of core-periphery structures in the European Union: A complexity perspective. Working Paper 6, ZOE Discussion Papers.

Gräbner, C., Heimberger, P., Kapeller, J., and Schütz, B. (2020). Is the Eurozone disintegrating? Macroeconomic divergence, structural polarisation, trade and fragility. *Cambridge Journal of Economics*, 44(3):647–669.

Jaynes, E. T. (2019). *Probability Theory: The Logic of Science*. Cambridge University Press.

Kalecki, M. (1945). On the Gibrat Distribution. *Econometrica*, 13(2):161–170.

Mundt, P., Förster, N., Alfarano, S., and Milaković, M. (2014). The real versus the financial economy: A global tale of stability versus volatility. *Economics: The Open-Access, Open-Assessment E-Journal*, 8(2014-17):1–26.

Prebisch, R. (1950). The economic development of Latin America and its principal problems. Sede de la CEPAL en Santiago (Estudios e Investigaciones), Naciones Unidas Comisión Económica para América Latina y el Caribe (CEPAL).

Raymond, R. (1999). The Euro, a New Currency for Europe and the World. *The Brown Journal of World Affairs*, 6(2):125–134.

Scharfenaker, E. and Semieniuk, G. (2015). A Mixture Model for Filtering Firms' Profit Rates. In *Bayesian Statistics from Methods to Models and Applications*, Springer Proceedings in Mathematics & Statistics, pages 153–164. Springer International Publishing.

Schulz, J. and Milaković, M. (2021). How Wealthy are the Rich? *Review of Income and Wealth*, forthcoming.

Shannon, C. E. (1948). A Mathematical Theory of Communication. *Bell System Technical Journal*, 27(3):379–423.

Shibuya, N. (2021). Normal Distribution Demystified. https://naokishibuya.medium.com/normal-distribution-demystified-933cf72185d2.

Singer, H. W. (1950). The Distribution of Gains between Investing and Borrowing Countries. *The American Economic Review*, 40(2):473–485.

Stan Development Team (2021). RStan: The R interface to Stan.

Thurner, S., Hanel, R. A., and Klimek, P. (2018). *Introduction to the Theory of Complex Systems*. Oxford University Press, Oxford : New York.

Zhao, J. (2021). Investigating the Asymmetric Core/Periphery Structure of International Labor Time Flows: A New Network Approach to Studying the World-System. *Journal of World - Systems Research*, 27(1):231–264.

A Solution to the Maximum Entropy Problem

We do not want to simply state the problem and solution to the Maximum Entropy problem but also explicitly outline the detailed process to derive the solution.

$$\begin{aligned}\mathcal{L}\left(p(x), \lambda_i\right) = &- \int_{-\infty}^{\infty} p(x) \times \log p(x) dx - \lambda_1 \left(\int_{-\infty}^{\infty} p(x) dx - 1 \right) \\ &- \lambda_2 \left(\int_{-\infty}^{\infty} p(x) \log x dx - \mu \right) - \lambda_3 \left(\int_{-\infty}^{\infty} p(x) \left(\log x - \mu \right)^2 dx - \sigma^2 \right)\end{aligned}$$

We can neglect the second secondary constraint, here indicated by $\lambda_2 \left(\int_{-\infty}^{\infty} p(x) \log x dx - \mu \right)$. The reason for that is that it is incorporated into the third secondary constraint where we define the second moment based on the first moment (**?**). We, therefore, have left:

$$\begin{aligned}\mathcal{L}\left(p(x), \lambda_i\right) = &- \int_{-\infty}^{\infty} p(x) \times \log p(x) dx - \lambda_1 \left(\int_{-\infty}^{\infty} p(x) dx - 1 \right) \\ &- \lambda_3 \left(\int_{-\infty}^{\infty} p(x) \left(\log x - \mu \right)^2 dx - \sigma^2 \right)\end{aligned}$$

First order solutions:

$$\begin{aligned}\frac{\partial \mathcal{L}}{\partial \lambda_1} &= \int_{-\infty}^{\infty} p(x) dx - 1 &&\stackrel{!}{=} 0 \\ \frac{\partial \mathcal{L}}{\partial \lambda_3} &= \int_{-\infty}^{\infty} p(x) \left(\log x - \mu \right)^2 dx - \sigma^2 &&\stackrel{!}{=} 0 \\ \frac{\partial \mathcal{L}}{\partial p(x)} &= -\log\left(p(x)\right) - 1 - \lambda_1 - \lambda_3 \left(\log(x) - \mu \right)^2 &&\stackrel{!}{=} 0\end{aligned}$$

We can rearrange $\frac{\partial \mathcal{L}}{\partial p(x)}$ to define $p(x)$:

$$p\left(x\right) = \exp\left(-1 - \lambda_1 - \lambda_3 \left(\log(x) - \mu \right)^2 \right)$$

Plugging this into the normalization constraint $\int_{-\infty}^{\infty} p(x) dx = 1$ gives us:

$$\begin{aligned}\int_{-\infty}^{\infty} p(x) dx &= \int_{-\infty}^{\infty} \exp\left(-1 - \lambda_1 - \lambda_3 \left(\log(x) - \mu \right)^2 \right) dx \\ &= 1\end{aligned}$$

In order to solve the problem we substitute z for $\sqrt{\lambda_3}\left(\log\left(x\right)-\mu\right)$, so that:

$$\begin{aligned} z &= \sqrt{\lambda_3}\left(\log\left(x\right)-\mu\right) \\ z^2 &= \lambda_3\left(\log\left(x\right)-\mu\right)^2 \\ dz &= \sqrt{\lambda_3}\frac{1}{x}dx \\ \Rightarrow dx &= \frac{x}{\sqrt{\lambda_3}}dz \end{aligned}$$

Applying this substitution gives the following expression:

$$\begin{aligned} \int_{-\infty}^{\infty} p(x)dx &= \int_{-\infty}^{\infty} \exp\left(-1-\lambda_1-\lambda_3\left(\log(x)-\mu\right)^2\right)dx \\ &= \int_{-\infty}^{\infty} \exp\left(-1-\lambda_1-z^2\right)\frac{x}{\sqrt{\lambda_3}}dz \\ &= \frac{\exp\left(-1-\lambda_1\right)x}{\sqrt{\lambda_3}}\int_{-\infty}^{\infty}\exp\left(-z^2\right)dz \\ &= \frac{\exp\left(-1-\lambda_1\right)x}{\sqrt{\lambda_3}}\sqrt{\pi} \end{aligned}$$

The last step in the previous equations is the application of the Gaussian integral. The Gaussian integral solves $\int_{-\infty}^{\infty}\exp\left(-z^2\right)dz$ for $\sqrt{\pi}$. We can now write and rearrange:

$$\begin{aligned} p\left(x\right) &= \exp\left(-1-\lambda_1\right)x\sqrt{\frac{\pi}{\lambda_3}} &&\stackrel{!}{=} 1 \\ \frac{1}{x}\sqrt{\frac{\lambda_3}{\pi}} &= \exp\left(-1-\lambda_1\right) \end{aligned}$$

We can use this result and plug it into the secondary constraint, which defines the second moment:

$$\begin{aligned} \sigma^2 &= \int_{-\infty}^{\infty} p(x)\left(\log x-\mu\right)^2 dx \\ &= \int_{-\infty}^{\infty} \exp\left(-1-\lambda_1-\lambda_3\left(\log(x)-\mu\right)^2\right)\left(\log x-\mu\right)^2 dx \\ &= \frac{1}{x}\sqrt{\frac{\lambda_3}{\pi}}\int_{-\infty}^{\infty}\exp\left(-\lambda_3\left(\log(x)-\mu\right)^2\right)dx \end{aligned}$$

We again substitute $z = \sqrt{\lambda_3}\left(\log\left(x\right) - \mu\right)$ and receive:

$$\begin{aligned}
\sigma^2 &= \frac{1}{x}\sqrt{\frac{\lambda_3}{\pi}}\int_{-\infty}^{\infty}\exp\left(-\lambda_3\left(\log(x)-\mu\right)^2\right)dx \\
&= \frac{1}{x}\sqrt{\frac{\lambda_3}{\pi}}\int_{-\infty}^{\infty}\exp\left(-z^2\right)\frac{z^2}{\lambda_3}\frac{dz}{\sqrt{\lambda_3}} \\
&= \frac{1}{x\lambda_3\sqrt{\pi}}\int_{-\infty}^{\infty}\exp\left(-z^2\right)z^2 dz \\
&= \frac{1}{x\lambda_3\sqrt{\pi}}\frac{\sqrt{\pi}}{2} \\
&= \frac{1}{2x\lambda_3}
\end{aligned}$$

We now have a solution for λ_3, which is $\frac{1}{2x\sigma^2}$, which we can plug into our previous calculations:

$$\begin{aligned}
\exp\left(-1-\lambda_1\right) &= \frac{1}{x}\sqrt{\frac{\lambda_3}{\pi}} \\
&= \frac{1}{x\sigma\sqrt{2\pi}}
\end{aligned}$$

We now have all the necessary parts to express the solution for $p\left(x\right)$:

$$\begin{aligned}
p\left(x\right) &= \exp\left(-1-\lambda_1-\lambda_3\left(\log(x)-\mu\right)^2\right) \\
&= \frac{1}{x\sigma\sqrt{2\pi}}\exp\left(-\frac{\left(\log\left(x\right)-\mu\right)^2}{2\sigma^2}\right)
\end{aligned}$$

The final equation is the probability density function for the log-normal distribution, and we have completed our goal.

B Maps of belonging

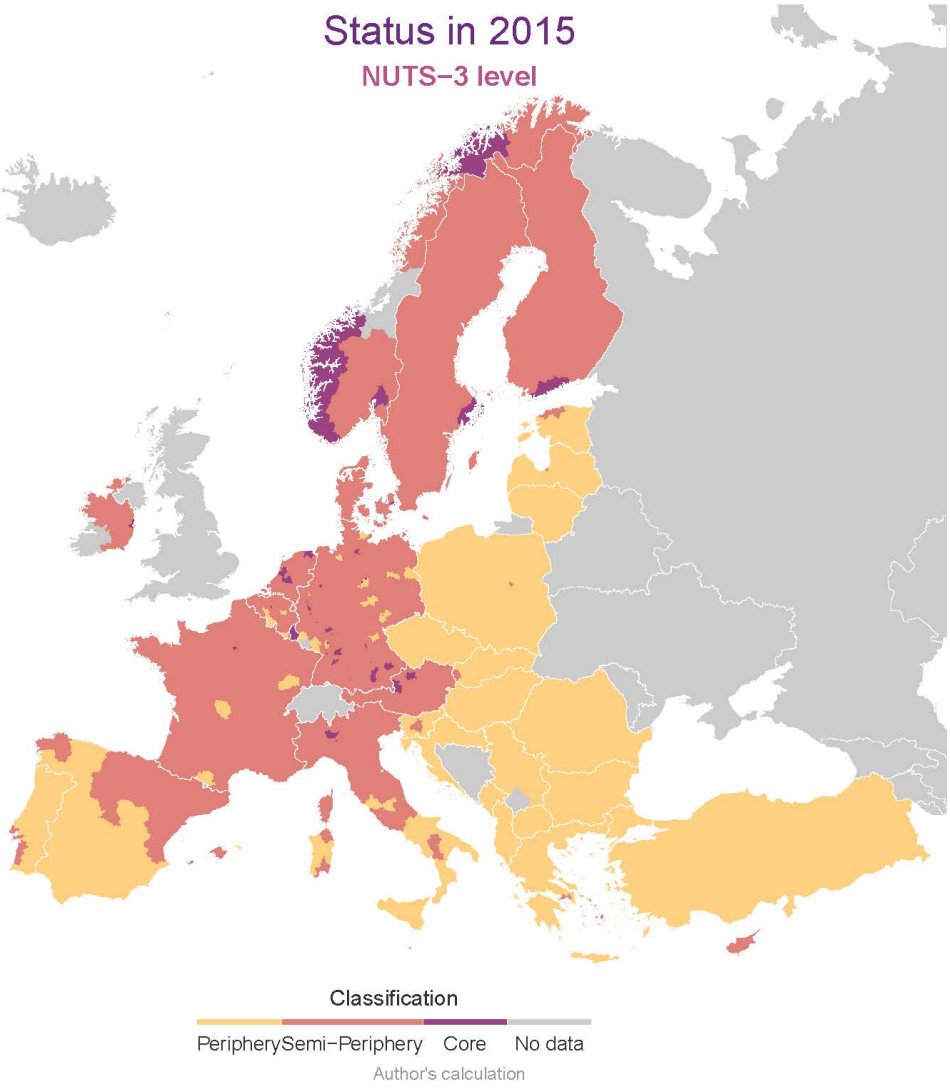

(a)

Figure 6: Visualization of the regions under consideration and their classification into core, semi-periphery, or periphery for the year 2015.

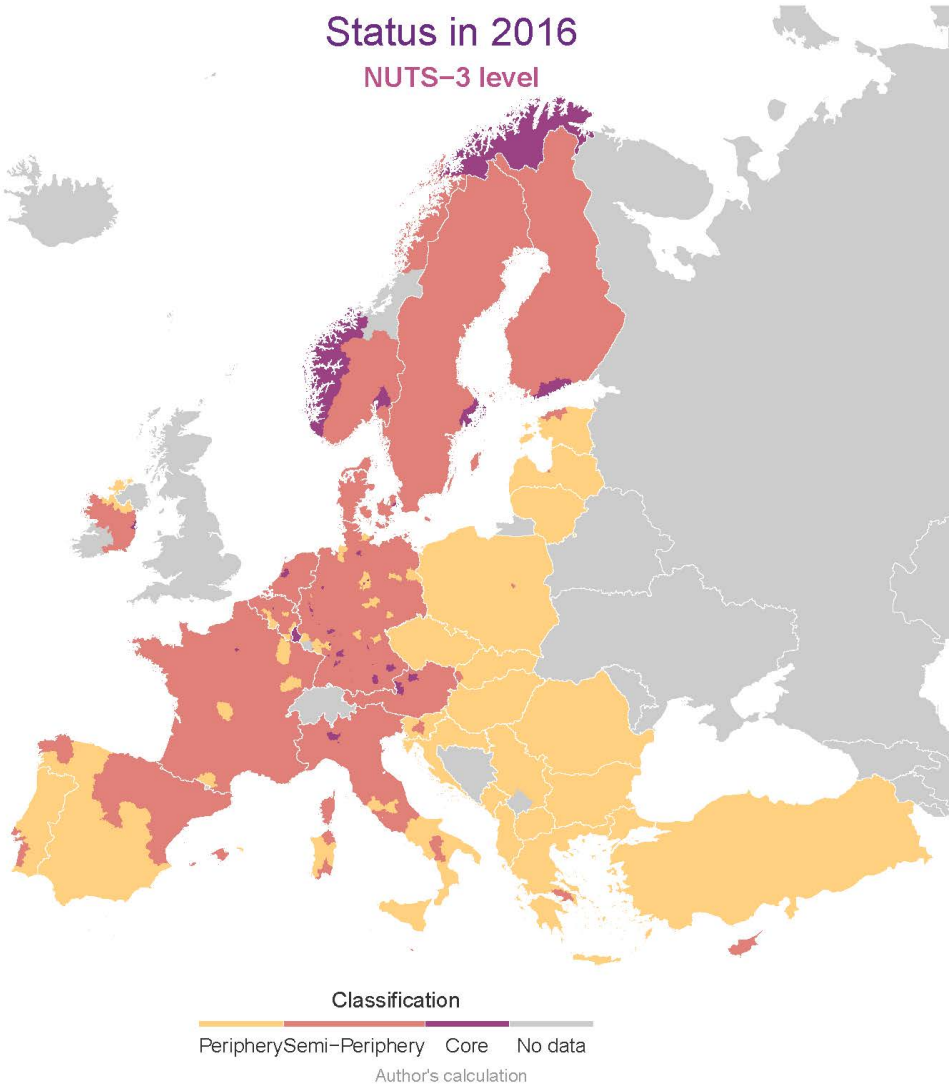

(a)

Figure 7: Visualization of the regions under consideration and their classification into core, semi-periphery, or periphery for the year 2016.

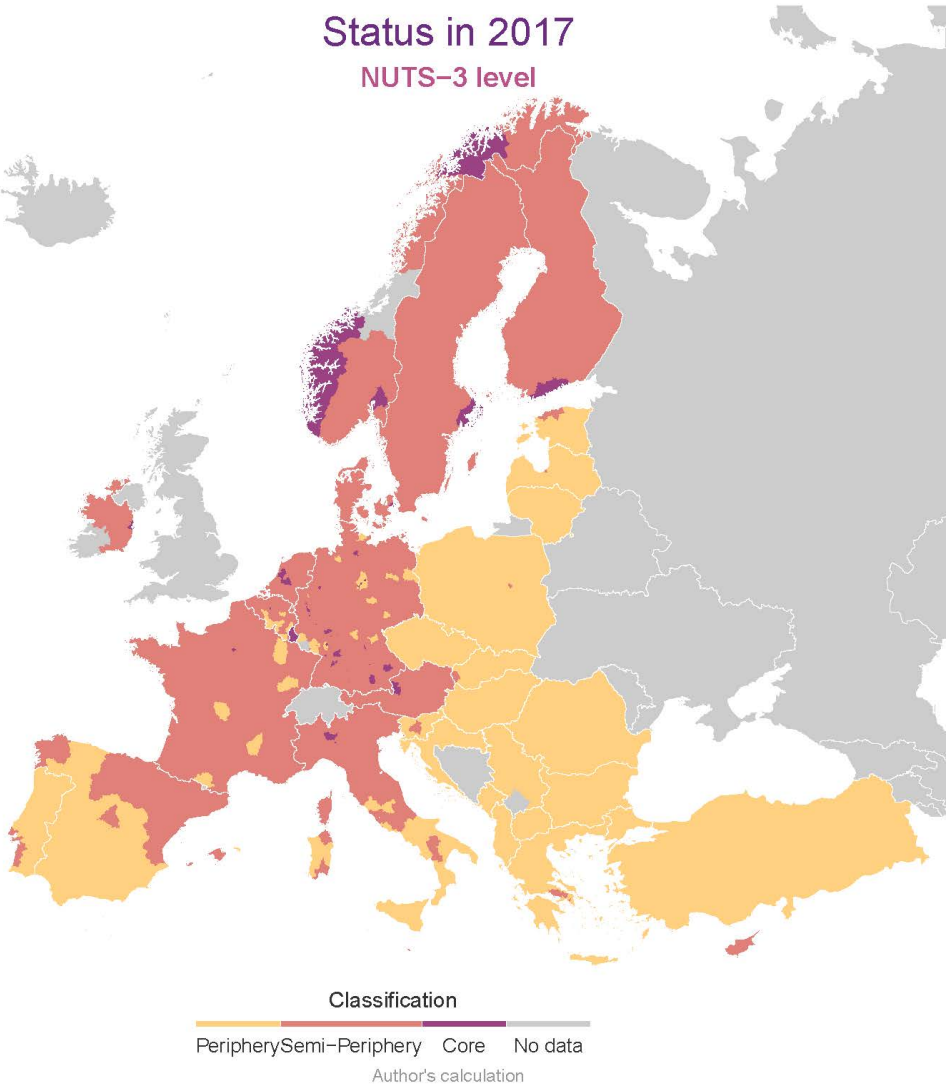

(a)

Figure 8: Visualization of the regions under consideration and their classification into core, semi-periphery, or periphery for the year 2017.